Ces1d deficiency protects against high-sucrose diet-induced hepatic triacylglycerol accumulation

Jihong Lian[1,2], Russell Watts[1,2], Ariel D. Quiroga[3], Megan R. Beggs[4], R. Todd Alexander[2,4], and Richard Lehner[1,2,5]

[1]Group on Molecular and Cell Biology of Lipids, University of Alberta, Alberta, Canada

[2]Department of Pediatrics, University of Alberta, Alberta, Canada

[3]Instituto de Fisiología Experimental (IFISE), Área Morfología, Facultad de Ciencias Bioquímicas y Farmacéuticas, CONICET, UNR, Rosario, Argentina.

[4]Department of Physiology, University of Alberta, Alberta, Canada

[5]Department of Cell Biology, University of Alberta, Alberta, Canada

To whom correspondence should be addressed:

Richard LEHNER, PhD, University of Alberta, Edmonton, AB, Canada T6G 2S2

Tel.: (780) 492-2963; Fax: (780) 492-3383; E-mail: richard.lehner@ualberta.ca

ABSTRACT

Non-alcoholic fatty liver disease (NAFLD) is the most common chronic liver disease. TG accumulation in liver is a hallmark of NAFLD. Metabolic studies have confirmed that increased hepatic *de novo* lipogenesis in humans contributes to fat accumulation in the liver and to NAFLD progression. Mice deficient in carboxylesterase 1d (Ces1d) expression are protected from high-fat diet-induced hepatic steatosis. To investigate whether loss of Ces1d can also mitigate steatosis induced by over-activated *de novo* lipogenesis, wild type and Ces1d deficient mice were fed a lipogenic high-sucrose diet. We found that Ces1d deficient mice were protected from high-sucrose diet-induced hepatic lipid accumulation. Mechanistically, Ces1d deficiency leads to activation of AMP-activated protein kinase and inhibitory phosphorylation of acetyl-CoA carboxylase. Together with our previous demonstration that Ces1d deficiency attenuated high-fat diet-induced steatosis, this study suggests that inhibition of CES1 (the human ortholog of Ces1d) might represent a novel pharmacological target for prevention and treatment of NAFLD.

Keywords: Carboxylesterase, high-sucrose diet, lipase, liver, triacylglycerol, NAFLD, lipogenesis

INTRODUCTION

Nonalcoholic fatty liver disease (NAFLD) is a chronic liver disorder that is increasing in prevalence with the global epidemic of obesity in adults and children (1, 2). Hepatic steatosis results from an imbalance between import, synthesis, utilization, and/or export of lipids. Considerable evidence supports the ability of high carbohydrate diets to upregulate hepatic *de novo* lipogenesis (DNL), leading to increased triacylglycerol (TG) production (3). Over-consumption of simple carbohydrates in processed foods and beverages, especially fructose and sucrose, has been implicated in NAFLD development (4, 5). Metabolites generated during carbohydrate metabolism in the liver serve as substrates for DNL and activate the master transcription factor carbohydrate-responsive element-binding protein (ChREBP) to induce mRNA expression of lipogenic genes, including genes encoding fatty acid synthase (FAS) and stearoyl-CoA desaturase 1 (SCD1) (6).

Our laboratory has investigated the role of carboxylesterases in lipid metabolism, including murine carboxylesterase 1d (Ces1d) [previously annotated as carboxylesterase 3 (Ces3) and triacylglycerol hydrolase (TGH)] (7-9). Ces1d was shown to participate in basal lipolysis in adipocytes (10, 11). In the liver, experimental evidence suggests that murine Ces1d and its human ortholog CES1 participate in the mobilization of preformed TG for very low-density lipoprotein (VLDL) assembly (12-15). Loss of Ces1d enhances insulin sensitivity and protects from high-fat diet-induced liver steatosis by increasing fatty acid (FA) oxidation and decreasing hepatic *de novo* lipogenesis (16). To specifically investigate whether ablation of *Ces1d* expression can alleviate steatosis induced by over-activated lipogenesis, we challenged Ces1d deficient mice with a high-sucrose diet. Here we show that Ces1d deficiency protects against high-carbohydrate-induced liver lipid accumulation by inhibiting the key lipogenic enzyme acetyl-CoA carboxylase (ACC).

MATERIALS AND METHODS

Animal care and diet studies

All animal procedures were conducted in compliance with protocols approved by the University of Alberta's Animal Care and Use Committee and in accordance with the Canadian Council on Animal Care policies and regulations. Sixteen weeks old male Ces1d deficient mice ($Ces1d^{-/-}$) and wild-type (WT) mice of C57BL/6J background were used in the experiments (16). WT and $Ces1d^{-/-}$ mice were maintained on a 12-hour light (7 am - 7 pm)/12-hour dark (7 pm - 7 am) cycle, controlled for temperature and humidity and were fed either a chow diet (5% fat and 0.02% cholesterol PicoLab laboratory Rodent Diet 5L0D) or a high-sucrose diet (HSD, no. 901683; 74% kcal from sucrose, fat-free, MP Biomedical, USA, supplemental Table S1) for 8 weeks. Blood and tissues were collected after 16 hours fasting or after 16 hours fasting followed by 6 hours re-feeding.

Metabolic measurements

Energy expenditure and fuel oxidation were assessed using the Oxymax CLAMS (Columbus Instruments USA). Mice were acclimated in individual chambers for one day before data recording. Measurements of *in vivo* oxygen consumption and carbon dioxide production were performed every 14 min over 2 days and used to calculate the respiratory exchange ratio (RER). Food intake was monitored during the procedure.

Body composition measurements

Whole body lean and fat masses were determined in mice by an EchoMRI™ system (USA) before and after 8 weeks of HSD feeding.

Plasma and liver chemistries

Enzymatic assays kits were used to measure plasma levels of free fatty acids (FFA), TG and ketone bodies (Wako, Japan) according to manufacturer's instructions. Plasma insulin concentration was determined using the Multiplexing LASER Bead Assay (Eve Technologies, Canada). Lipid profile was determined in liver homogenates (1 mg of protein) by gas

4

chromatography (GC) as previously described (17). Hepatic fatty acid composition and concentration were determined by GC analysis following transesterification of fatty acids present in total liver lipid extract to fatty acid methyl esters in the presence of 17C-fatty acid as an internal standard (10). Liver glycogen was determined by a Glycogen Assay Kit (Sigma-Aldrich, USA) according to manufacturer's instructions. Blood gases (pH, HCO_3, PCO_2) were tested by i-STAT handheld blood analyzer with the EC8+ cartridges (Abbott, US) (18).

In vivo VLDL-TG secretion

Mice were fasted overnight and then injected intraperitoneally (I.P.) with Poloxamer 407 (1 g/kg body weight). Blood was collected before and 1, 2, and 3 hours after injection. TG concentration was determined by a kit assay (Roche Diagnostics GmbH, Germany).

Immunoblot analyses

Livers were homogenized in sucrose buffer (250 mM sucrose, 50 mM Tris, 1 mM EDTA, pH 7.4), separated by SDS-polyacrylamide gels and transferred to polyvinylidene difluoride (PVDF) membranes (catalog # IPVH00010, Millipore). Antibodies used in this study include anti-adipose triglyceride lipase (ATGL) (catalog # 2138, Cell Signaling, USA), anti-fatty acid synthase (FAS) (catalog # 3180, Cell Signaling), anti-stearoyl-CoA desaturase 1 (SCD1) (catalog # 2794, Cell Signaling), anti-perilipin 2 (Plin2) (catalog # LS-B7983, LifeSpan BioSciences, USA), anti-perilipin 5 (PLIN5) (catalog # GP31, PROGEN, Germany), anti-α/β hydrolase domain 5/comparative gene identification-58 (ABHD5/CGI-58) (catalog # 12201-1-AP, Proteintech, USA), anti-adipose triglyceride lipase (ATGL) (catalog # 2138, Cell Signaling, USA), anti-cell death-induced DFF45-like effector B (CIDEB) (a gift from Dr. Peng Li, Tsinghua University, China), anti-phospho-AMP-activated protein kinase (pAMPK) and AMPK (catalog #'s 2531 and 2532, respectively, Cell Signaling), anti-phospho-ACC (pACC) and ACC (catalog #'s 3661 and 3662, respectively, Cell Signaling), anti-phospho-HSL (pHSL) and HSL (catalog #'s 4126 and 4107, respectively, Cell Signaling). Reactivity was detected by enhanced chemiluminescence, and

5

visualized by G:BOX system (SynGene, UK). The relative intensities of resulting bands on the blots were analyzed by densitometry using GeneTools program (SynGene).

RNA isolation and real-time qPCR analysis

Total liver RNA was isolated using Trizol reagent (Invitrogen, USA). First-strand cDNA was synthesized from 2 μg total RNA using Superscript III reverse transcriptase (Invitrogen) primed by oligo $(dt)_{12-18}$ (Invitrogen) and random primers (Invitrogen). Real-time qPCR was performed with Power SYBR® Green PCR Master Mix kit (Life Technologies, UK) using the StepOnePlus-Real time PCR System (Applied Biosystems, Canada). Data were analyzed with the StepOne software (Applied Biosystems). Standard curves were used to calculate mRNA abundance relative to that of a control gene, cyclophilin. Real-time qPCR primers are summarized in the supplemental Table S2. All primers were synthesized by Integrated DNA Technologies (Canada).

In vivo lipogenesis

In vivo lipogenesis with acetate as precursor substrate was performed as described before with some modifications (19). In brief, mice fed HSD for 8 weeks were fasted overnight before re-feeding for 6 hours,, then 30 μCi of ^{14}C-acetate was I.P. injected into each mouse. Liver and white adipose tissue (WAT) were harvested 1 h after injection. For liver lipid analysis, lipids were exacted from tissues, separated on thin layer chromatography (TLC) plates with hexane:isopropyl ether:acetic acid (15:10:1, v/v/v), visualized by exposure to iodine. Radioactivity in the resolved lipid classes was determined by scintillation counting. For the WAT, radioactivity was measured in the total lipid extracts by scintillation counting.

Glucose tolerance test

Mice were fasted for 16 hours prior to oral gavage of glucose (2 g/kg). Plasma levels of glucose were monitored at the indicated time points using glucose strips (Accu-Check glucometer, Roche Diagnostics, Vienna, Austria).

Statistics

All values are expressed as mean ± SEM. Significant difference between two groups was

6

determined by unpaired 2-tailed t test. Data from studies in WT and $Ces1d^{-/-}$ mice fed on chow diet and HSD were analyzed by two-way ANOVA followed by Bonferroni post-test (GraphPad PRISM 6 software). Differences were considered statistically significant at $*P < 0.05$, $**P < 0.01$, $***P < 0.001$.

RESULTS

Effects of Ces1d deficiency on whole body metabolism in mice fed high sucrose diet

Sixteen weeks old $Ces1d^{-/-}$ and WT mice were fed with HSD or standard chow diet for 8 weeks. WT mice did not show difference in body weight between chow and HSD feeding conditions (Figure 1A). Although $Ces1d^{-/-}$ mice trended towards a heavier body weight at the beginning of the diet-feeding period (Figure 1A), during the 8 weeks feeding the body weight increment was blunted in $Ces1d^{-/-}$ mice on both chow diet and HSD. After 8 weeks of feeding no difference in body weight was observed between Ces1d deficient and WT mice on either diet (Figure 1A). Weight gain curve before the initiation of dietary intervention suggests that $Ces1d^{-/-}$ mice fed a regular chow diet reach adult body weight earlier than WT mice during the life phase as mature adults (supplemental Figure S1A). $Ces1d^{-/-}$ mice fed HSD tended to lose weight compared with the $Ces1d^{-/-}$ mice fed a regular chow diet (Figure 1A). $Ces1d^{-/-}$ mice had less epididymal WAT weight and/or lower WAT/body weight ratio on both chow diet and HSD (Figure 1B). MRI scans showed no difference in body composition of fat and lean mass percentage in WT and $Ces1d^{-/-}$ mice before HSD feeding. HSD feeding increased body fat percentage and decreased lean percentage in the WT mice, but this change was not observed in $Ces1d^{-/-}$ mice (supplemental Figure S1B and S1C). These data suggest that the lower weight gain observed in the $Ces1d^{-/-}$ mice could be at least partially derived from decreased WAT depots compared to WT mice.

The 16-hour fasting FFA concentration in $Ces1d^{-/-}$ mice either decreased (chow diet) or did not change (HSD) compared with WT control groups (Figure 1C). $Ces1d^{-/-}$ mice in the HSD group showed reduced plasma FFA concentration in the refed state (Figure 1C), which could be due to

7

decreased Ces1d-catalyzed basal lipolysis in Ces1d$^{-/-}$ adipocytes (10, 11). Collectively, these data suggest that the decreased fat depot in Ces1d$^{-/-}$ mice fed HSD is not due to increased lipolysis in adipose tissue. Consistent with this observation, plasma ketone body concentration was decreased in the *Ces1d$^{-/-}$* mice on both diets (Figure 1D), reflecting decreased FA utilization. Blood pH, acid and gases were also monitored in this study and no difference was observed between genotypes in either diet condition (Figure 1E), which confirms that the acid-base balance in the blood was not affected neither by the diets nor by the genotype.

Ces1d$^{-/-}$ mice consumed more chow diet than WT mice during the dark phase but no significant differences were observed in HSD intake between WT and *Ces1d$^{-/-}$* mice (supplemental Figure S2). As expected, the respiratory exchange ratio (RER) values were elevated in both *Ces1d$^{-/-}$* and WT mice after HSD feeding (Figure 1F), reflecting an increased utilization of carbohydrates as the energy source. *Ces1d$^{-/-}$* mice showed increased RER values when fed both the chow diet or HSD compared to the WT control groups (Figure 1F), indicating more reliance on carbohydrate over fat as energy source. There was no difference in energy expenditure between *Ces1d$^{-/-}$* and WT mice after HSD feeding (data not shown).

Amelioration of HSD-induced liver lipid accumulation in Ces1d deficient mice

To determine if Ces1d deficiency can protect against steatosis induced by DNL, analyses were performed on livers collected after refeeding when DNL is activated. HSD feeding increased liver weight in WT mice but not in *Ces1d$^{-/-}$* mice (Figure 2A). As expected, HSD induced an increment in hepatic TG content in WT mice; however, HSD had no effect on hepatic TG content in *Ces1d$^{-/-}$* mice with TG concentrations not differing from chow-fed *Ces1d$^{-/-}$* mice (Figure 2B). HSD feeding also increased liver cholesteryl ester (CE) and free cholesterol (FC) concentrations in both WT and *Ces1d$^{-/-}$* mice (Figure 2C and D). Liver FC concentration in HSD-fed *Ces1d$^{-/-}$* mice was slightly, but significantly decreased compared to WT mice (Figure 2D).

Considering that the HSD utilized in this study was a fat-free diet, which could potentially lead to essential fatty acid (EFA) deficiency, hepatic fatty acid composition in total lipid extract was

determined. After 8 weeks of HSD feeding, both WT and *Ces1d*^{-/-} mice showed similar decrease in hepatic concentration of linoleic acid and α-linolenic acid, and their long-chain metabolites arachidonic acid, eicosapentaenoic acid, and docosahexaenoic acid (supplemental Figure S3 A-E), Oleic acid that can be synthesized in the liver, was increased by HSD feeding in both genotypes, although the increment in *Ces1d*^{-/-} mice was significantly lower in WT mice (supplemental Figure S3 F), which is consistent with the obtained liver lipid profiles (Figure 2B) and may be the consequence of attenuated TG synthesis.

HSD feeding slightly increased hepatic mRNA expression of pro-inflammatory genes *F4/80* and *Cd68*, but no differences were found between WT and *Ces1d*^{-/-} mice (supplemental Figure S4).

No difference was observed in plasma TG concentration between WT and *Ces1d*^{-/-} mice fed HSD (Figure 2E). VLDL-TG secretion rate was not altered in the four groups of animals (supplemental Figure S5), suggesting that the difference in the liver lipid profile was not caused by altered VLDL secretion.

Ces1d deficiency regulates liver lipid metabolism through a posttranscriptional mechanism

Carbohydrate response element binding protein (ChREBP) is activated by carbohydrate metabolites leading to up-regulated transcription of genes encoding lipogenic enzymes and consequently increased DNL in the liver (6). Two ChREBP isoforms, ChREBP-α and ChREBP-β have been characterized. A two-step model has been proposed for ChREBP activation, by which carbohydrate-mediated activation of ChREBP-α induces expression of the ChREBP-β isoform (20). In the current study, HSD feeding dramatically increased hepatic expression of *Mlxipl (beta)* encoding the ChREBP-β isoform in both WT and *Ces1d*^{-/-} mice at a comparable level (Figure 3A and B). Consequently, hepatic expression of ChREBP target genes *Pklr* (encoding liver pyruvate kinase) and *Txnip* (encoding thioredoxin-interacting protein) was induced in HSD-fed mice with no difference observed between WT and *Ces1d*^{-/-} mice (Figure 3C and D). These results suggest that ablation of *Ces1d* expression does not affect the regulation of lipogenic gene expression by hepatic ChREBP.

9

Liver X receptor (LXR) increases transcription of lipogenic genes by activating sterol regulatory element-binding protein-1c (SREBP1c), another important regulatary transcription factor of DNL (21). Glucose and its derivatives were demonstrated to induce LXR transcriptional activity (22, 23). In the present study the expression of *Nr1h3* gene encoding LXRα was not changed by genotype or diet type (Figure 3E), while the LXRα target gene *Abca1* was slightly induced by HSD feeding (Figure 3F), suggesting activation of LXR by over-consumption of sugar. Expression of LXRα target gene *Abca1* was comparable between WT and *Ces1d*$^{-/-}$ mice on both types of diet, which suggests that the attenuated liver lipid accumulation in *Ces1d*$^{-/-}$ mice was not due to changes in LXR-mediated transcriptional activity.

Consistent with previous studies (24, 25), high-carbohydrate diet elevated expression of *Srebf1* in the liver of WT and *Ces1d*$^{-/-}$ mice (Figure 3G). Compared with WT mice, *Ces1d*$^{-/-}$ mice presented with attenuated *Srebf1* expression in the liver. However, the SREBP1c target lipogenic enzymes FAS and SCD1 did not exhibit different protein abundance between WT and *Ces1d*$^{-/-}$ groups (Figure 4A and B). Expression of another key enzyme of lipogenesis, ACC was induced by HSD feeding to a comparable level in both WT and *Ces1d*$^{-/-}$ mice (Figure 4C). However, phosphorylation state of ACC (p-ACC) was significantly higher in *Ces1d*$^{-/-}$ mice compared to the WT groups in both diet conditions, suggesting suppressed liver ACC activity in *Ces1d*$^{-/-}$ mice (Figure 4C), which may contribute to the attenuated liver TG accumulation after HSD feeding. It is well established that AMPK catalyzes ACC phosphorylation, thereby inhibiting ACC activity and DNL (26, 27). In agreement with this canonical regulation, increased phosphorylated state of AMPK (p-AMPK) in the livers of *Ces1d*$^{-/-}$ mice suggests higher AMPK activity (Figure 4D).

HSD feeding also increased the abundance of SCD1 and ACC but not FAS in the WAT. No difference was found between WT and *Ces1d*$^{-/-}$ mice (supplemental Figure S6A and B). Furthermore, P-ACC/ACC and P-AMPK/AMPK ratios also did not change in WAT between WT and *Ces1d*$^{-/-}$ mice (supplemental Figure S6B), suggesting that the effect of Ces1d deficiency on phosphorylated states of ACC and AMPK are liver specific.

10

DNL was further assessed by incorporation of [^{14}C]-labeled acetate into lipids in HSD-fed WT and $Ces1d^{-/-}$ mice in the refed state. No difference was observed in the incorporation of the radioisotope into TG, CE and cholesterol in the liver (supplemental Figure S7), suggesting that lipids synthesized from acetate-derived substrate in the liver are comparable between HSD fed WT and $Ces1d^{-/-}$ mice. The incorporation of acetate into total lipids in WAT also did not vary between HSD-fed WT and $Ces1d^{-/-}$ mice (supplemental Figure S6C).

Hepatic expression of FA oxidation related genes *Cpt1a* (encoding carnitine palmitoyltransferase 1A) and *Acox* (encoding acyl-CoA oxidase) did not differ between genotypes or diet types after fasting (Figure 5A). To investigate whether the attenuated TG accumulation in the liver of $Ces1d^{-/-}$ mice could be attributed to changes in LD-associated lipase abundance/activity, hepatic expression of ATGL and its regulators was assessed. The mRNA expression of *G0s2*, encoding an inhibitor of ATGL (28), was decreased in livers of $Ces1d^{-/-}$ mice fed chow diet when compared with the WT group on the same diet, however, no significant difference was seen between the two HSD fed groups (Figure 5B). It has been demonstrated that LD coat proteins perilipin 2 (PLIN2) and perilipin 5 (PLIN5) block ATGL-mediated lipolysis in the liver (29, 30). PLIN2 and PLIN5 abundance did not differ between the genotypes (Figure 5C). Abundance of ATGL coactivator ABHD5/CGI-58 also did not differ between WT and $Ces1d^{-/-}$ mice fed either chow diet or HSD (Figure 5C). Similar protein abundance of ATGL was found between WT and $Ces1d^{-/-}$ groups (Figure 5D). Hormone sensitive lipase (HSL) is also involved in liver lipolysis (31) and its activity is elevated by phosphorylation through PKA pathway and inhibited by dephosphorylation through insulin signaling (32). The phosphorylation state of liver HSL did not differ between HSD fed WT and $Ces1d^{-/-}$ mice (supplemental Figure S8). These results suggest that the attenuation of HSD-induced liver TG accumulation observed in $Ces1d^{-/-}$ mice was independent of cytosolic lipase activity in the liver.

Additional regulators of LD dynamics were investigated. The CIDE protein family, including CIDEA, CIDEB, and CIDEC/Fsp27, was demonstrated to be associated with LDs and promote

11

LD growth (33). Among the three isoforms, CIDEB is prominently expressed in the liver and intestine (33). CIDEB knockout mice exhibit resistance to high-fat diet induced steatosis (34). The expression of CIDEA and CIDEC is more abundant in the adipose tissue, while their hepatic expression is induced in fatty liver and positively correlates with the severity of liver steatosis (33, 35, 36). *Cidea* and *Cidec* expression levels were variable with *Cidea* trending towards an increase in livers of HSD fed WT but not $Ces1d^{-/-}$ mice (Figure 5E), which could be the result of HSD feeding only inducing mild lipid accumulation in the liver (Figure 2B). *Cideb* expression was slightly but significantly induced by HSD in WT mice, whereas *Cideb* expression in HSD fed $Ces1d^{-/-}$ mice was reduced compared to WT mice and did not statistically differ from chow-fed WT and $Ces1d^{-/-}$ mice (Figure 5E). Similar protein expression pattern of liver CIDEB among groups was observed by immunoblotting (Figure 5D).

Fibroblast growth factor 21 (FGF21), an endocrine hormone produced by liver, plays an important role in the maintenance of lipid and energy homeostasis. Previous studies have demonstrated that hepatic FGF21 expression increases in response to HSD or sucrose challenge (37, 38). HSD elevated expression of *Fgf21* in livers of both WT and $Ces1d^{-/-}$ mice with comparable levels (Figure 5F), suggesting the changes in energy and lipid metabolism observed in $Ces1d^{-/-}$ mice were not due to regulation by FGF21.

Glucose metabolism in Ces1d deficient mice fed HSD

Hepatic mRNA expression of key enzymes in gluconeogenesis has been determined. Decreased expression of glucose-6-phosphatase (*G6pc*) was found in $Ces1d^{-/-}$ mice fed HSD when compared to the WT control (Figure 6A). No alterations were observed in the expression of phosphoenolpyruvate carboxykinase (*Pck1*) between genotypes fed either diet (Figure 6A).

No difference in glucose tolerance was detected between WT and $Ces1d^{-/-}$ mice regardless of diet in the oral glucose tolerance test (OGTT) (Figure 6B). No significant difference was found in plasma insulin levels after refeeding between genotypes (Figure 6C). These data suggest that the whole body glucose metabolism in mice fed HSD was not affected by Ces1d deficiency.

12

Slightly increased hepatic glycogen concentration was observed in $Ces1d^{-/-}$ mice fed chow diet when compared to WT control mice, but no difference was observed between the two HSD fed groups (Figure 6D), suggesting that the attenuation of HSD-induced liver TG accumulation in $Ces1d^{-/-}$ mice was not due to a shift of sucrose derived metabolites from lipid synthesis to glycogen synthesis.

DISCUSSION

The prevalence of NAFLD in humans has increased with the rapid rise in carbohydrate consumption (39). The major finding in this study is that Ces1d deficiency prevents HSD-induced liver lipid accumulation *in vivo*.

DNL is one of the major sources of liver FA. NAFLD patients present with elevated hepatic DNL, which contributes to hepatic lipid accumulation (40). It is well documented that over-consumption of a high-carbohydrate diet, in particular simple sugars such as fructose and sucrose, dramatically induces hepatic DNL (41, 42) mainly through over-activation of lipogenesis master regulators ChREBP (6, 20) and SREBP1c (24, 25) and providing excess substrate for lipogenesis. In the present study, mice lacking Ces1d were protected from HSD feeding-induced liver TG accumulation. This occurred despite activation of both the ChREBP and SREBP1c pathways to a comparable level by HSD feeding in Ces1d deficient and WT control groups, suggesting that the attenuated hepatic TG accumulation observed in the Ces1d deficient mice was due to an alternative mechanism. Activities of a number of lipogenic enzymes are regulated by post-transcriptional mechanisms. AMPK has emerged as a key regulator of energy balance and plays an important role in regulating lipid and carbohydrate homeostasis. It has been well established that AMPK suppresses lipid synthesis through phosphorylation of key enzymes in FA and cholesterol biosynthesis pathways (26, 27, 43, 44). Activation of AMPK inhibits FA synthesis by phosphorylating ACC1 at Ser79 (45). Liver-specific activation of AMPK has been shown to decrease hepatic DNL and protect from high-fructose diet-induced steatosis (46). Increased

13

AMPK activation and ACC1 phosphorylation were observed in Ces1d deficient mice fed HSD. The mechanism by which AMPK is activated in livers of $Ces1d^{-/-}$ mice and how it is related to the changes in whole body metabolism (such as decreased fat deposition and increased RER) remains to be determined.

Despite decreased hepatic lipid concentration in HSD fed $Ces1d^{-/-}$ mice compared to WT mice, the abundance of LD-coat protein PLIN2 was not significantly different. It has been reported that AMPK catalyzes phosphorylation of PLIN2 thereby facilitates association of ATGL to LDs to catalyze lipolysis (47). This mechanism would be consistent with the observed increase in AMPK activation in livers of $Ces1d^{-/-}$ mice.

Ces1d and its human ortholog CES1 have been shown to play a role in the regulation of lipid metabolism (48). Ces1d participates in basal lipolysis in adipocytes (10, 11) and in the provision of substrates for the assembly of hepatic VLDL (8). The absence of Ces1d decreases VLDL secretion *in vivo* but does not cause liver steatosis (49), which may be at least partially attributable to decreased FA flux from adipose tissue to the liver in Ces1d knockout mice (49). Additionally, increased FA oxidation was observed in the Ces1d deficient hepatocytes and liver-specific Ces1d knockout mice (49, 50), which could also contribute to the prevention of liver lipid accumulation. We demonstrated in our previous study that ablation of Ces1d expression protects mice from high-fat diet-induced liver steatosis by decreasing hepatic DNL, increasing FA oxidation, and enhancing insulin sensitivity (16). Unlike our observations in the HSD fed Ces1d knockout mice, reduction of lipogenesis in $Ces1d^{-/-}$ mice after high-fat diet feeding was attributable to reduced expression of SREBP1c target enzymes including SCD1 and ACC instead of post-transcriptional regulation of the enzyme activity. The distinct mechanisms observed between the two studies could be explained by the different diets used. In the present study, although *Srebf1* mRNA abundance was decreased in the HSD fed $Ces1d^{-/-}$ mice, this change did not diminish the expression of target enzymes, which is likely due to the compensatory over-activation of ChREBP-mediated induction of lipogenic enzymes in the HSD feeding condition.

Increased liver FA oxidation was observed in the high-fat diet fed Ces1d deficient mice compared with the WT control mice fed the same diet (16). In the high-sucrose, fat-free diet- fed *Ces1d*^{-/-} mice, we did not observe enhanced levels of plasma ketone body concentration and expression of genes involved in FA oxidation in the liver in fasted state, which may be due to decreased FA flux to the liver and a shift towards carbohydrate as the primary energy source identified by the increased RER. Increased utilization of carbohydrates as the energy source in HSD feeding condition may also decrease the availability of substrates derived from carbohydrates for DNL in the liver of *Ces1d*^{-/-} mice, thus contributing to attenuated lipid synthesis. On the other hand, the decreased FA flux in the circulation may also contribute to reduced lipid storage in the livers of HSD fed *Ces1d*^{-/-} mice.

Decreased plasma TG was observed in chow fed *Ces1d*^{-/-} mice compared to WT mice under fasted state despite unchanged rate of VLDL-TG secretion. This is consistent with previous observations in *Ces1d*^{-/-} mice fed chow diet suggesting compensatory TG association with apoB48-containing lipoproteins (49, 51). In the current study, HSD feeding decreased plasma TG but did not affect VLDL secretion rate, and no difference was observed between *Ces1d*^{-/-} and WT mice, suggesting that the difference in liver lipid storage among animal groups was unlikely due to changes in VLDL assembly.

In vivo lipogenesis experiments using labeled acetate as the lipogenic substrate did not show differences in HSD fed WT and *Ces1d*^{-/-} mice during the refed state, when lipogenesis is most active. However, this result only demonstrates that lipid synthesis from acetate-derived substrate was not changed by Ces1d deficiency. HSD feeding increases acetyl-CoA flux from carbohydrate metabolism to lipogenesis (52). The RER data showed increased carbohydrate utilization in *Ces1d*^{-/-} mice over FA, which could result in different cytosolic acetyl-CoA pools between HSD fed WT and *Ces1d*^{-/-} mice and lead to reduced dilution by endogenous acetyl-CoA and increased acetyl-CoA specific radioactivity in *Ces1d*^{-/-} mice. Future studies should consider using other lipogenic substrates that would represent metabolism of carbohydrate.

15

In conclusion, HSD over-consumption leads to significantly enhanced DNL and lipid accumulation in the liver. Emerging evidence from recent epidemiological and biochemical studies suggest that high dietary intake of carbohydrate is an important causative factor in the development of metabolic syndrome features including NAFLD. Our data suggest that ablation of Ces1d activity reduces hepatic lipid accumulation, and therefore inhibition of the human ortholog CES1 might represent a novel pharmacological target for prevention and treatment of NAFLD.

Acknowledgments

Conflict of interest

The authors have declared that no conflict of interest exists.

REFERENCES

1. Bedogni, G., L. Miglioli, F. Masutti, C. Tiribelli, G. Marchesini, and S. Bellentani. 2005. Prevalence of and risk factors for nonalcoholic fatty liver disease: the Dionysos nutrition and liver study. *Hepatology*. **42**: 44-52.

2. Younossi, Z. M., A. B. Koenig, D. Abdelatif, Y. Fazel, L. Henry, and M. Wymer. 2016. Global epidemiology of nonalcoholic fatty liver disease-Meta-analytic assessment of prevalence, incidence, and outcomes. *Hepatology*. **64**: 73-84.

3. Kok, N., M. Roberfroid, and N. Delzenne. 1996. Dietary oligofructose modifies the impact of fructose on hepatic triacylglycerol metabolism. *Metabolism*. **45**: 1547-1550.

4. Nikpartow, N., A. D. Danyliw, S. J. Whiting, H. Lim, and H. Vatanparast. 2012. Fruit drink consumption is associated with overweight and obesity in Canadian women. *Can. J. Public. Health*. **103**: 178-182.

5. Malik, V. S., B. M. Popkin, G. A. Bray, J. P. Despres, and F. B. Hu. 2010. Sugar-sweetened beverages, obesity, type 2 diabetes mellitus, and cardiovascular disease risk. *Circulation*. **121**: 1356-1364.

6. Abdul-Wahed, A., S. Guilmeau, and C. Postic. 2017. Sweet Sixteenth for ChREBP: Established Roles and Future Goals. *Cell. Metab*. **26**: 324-341.

7. Lehner, R., and R. Verger. 1997. Purification and characterization of a porcine liver microsomal triacylglycerol hydrolase. *Biochemistry*. **36**: 1861-1868.

8. Lehner, R., and D. E. Vance. 1999. Cloning and expression of a cDNA encoding a hepatic microsomal lipase that mobilizes stored triacylglycerol. *Biochem. J.* **343 Pt 1**: 1-10.

9. Dolinsky, V. W., S. Sipione, R. Lehner, and D. E. Vance. 2001. The cloning and expression of a murine triacylglycerol hydrolase cDNA and the structure of its corresponding gene. *Biochim. Biophys. Acta*. **1532**: 162-172.

10. Wei, E., W. Gao, and R. Lehner. 2007. Attenuation of adipocyte triacylglycerol hydrolase activity decreases basal fatty acid efflux. *J. Biol. Chem.* **282**: 8027-8035.

11.	Dominguez, E., A. Galmozzi, J. W. Chang, K. L. Hsu, J. Pawlak, W. Li, C. Godio, J. Thomas, D. Partida, S. Niessen, P. E. O'Brien, A. P. Russell, M. J. Watt, D. K. Nomura, B. F. Cravatt, and E. Saez. 2014. Integrated phenotypic and activity-based profiling links Ces3 to obesity and diabetes. *Nat. Chem. Biol.* **10**: 113-121.

12.	Lehner, R., Z. Cui, and D. E. Vance. 1999. Subcellullar localization, developmental expression and characterization of a liver triacylglycerol hydrolase. *Biochem. J.* **338 (Pt 3)**: 761-768.

13.	Dolinsky, V. W., D. N. Douglas, R. Lehner, and D. E. Vance. 2004. Regulation of the enzymes of hepatic microsomal triacylglycerol lipolysis and re-esterification by the glucocorticoid dexamethasone. *Biochem. J.* **378**: 967-974.

14.	Gilham, D., S. Ho, M. Rasouli, P. Martres, D. E. Vance, and R. Lehner. 2003. Inhibitors of hepatic microsomal triacylglycerol hydrolase decrease very low density lipoprotein secretion. *FASEB. J.* **17**: 1685-1687.

15.	Gilham, D., M. Alam, W. Gao, D. E. Vance, and R. Lehner. 2005. Triacylglycerol hydrolase is localized to the endoplasmic reticulum by an unusual retrieval sequence where it participates in VLDL assembly without utilizing VLDL lipids as substrates. *Mol. Biol. Cell.* **16**: 984-996.

16.	Lian, J., E. Wei, J. Groenendyk, S. K. Das, M. Hermansson, L. Li, R. Watts, A. Thiesen, G. Y. Oudit, M. Michalak, and R. Lehner. 2016. Ces3/TGH Deficiency Attenuates Steatohepatitis. *Sci. rep.* **6**: 25747.

17.	Sahoo, D., T. C. Trischuk, T. Chan, V. A. Drover, S. Ho, G. Chimini, L. B. Agellon, R. Agnihotri, G. A. Francis, and R. Lehner. 2004. ABCA1-dependent lipid efflux to apolipoprotein A-I mediates HDL particle formation and decreases VLDL secretion from murine hepatocytes. *J. Lipid. Res.* **45**: 1122-1131.

18.	Pan, W., J. Borovac, Z. Spicer, J. G. Hoenderop, R. J. Bindels, G. E. Shull, M. R. Doschak, E. Cordat, and R. T. Alexander. 2012. The epithelial sodium/proton exchanger, NHE3,

is necessary for renal and intestinal calcium (re)absorption. *Am. J. Physiol. Renal. Physiol.* **302**: F943-956.

19.   Kita, K., M. Furuse, S. I. Yang, and J. Okumura. 1992. Influence of dietary sorbose on lipogenesis in gold thioglucose-injected obese mice. *Int. J. Biochem.* **24**: 249-253.

20.   Herman, M. A., O. D. Peroni, J. Villoria, M. R. Schon, N. A. Abumrad, M. Bluher, S. Klein, and B. B. Kahn. 2012. A novel ChREBP isoform in adipose tissue regulates systemic glucose metabolism. *Nature.* **484**: 333-338.

21.   Repa, J. J., G. Liang, J. Ou, Y. Bashmakov, J. M. Lobaccaro, I. Shimomura, B. Shan, M. S. Brown, J. L. Goldstein, and D. J. Mangelsdorf. 2000. Regulation of mouse sterol regulatory element-binding protein-1c gene (SREBP-1c) by oxysterol receptors, LXRalpha and LXRbeta. *Genes. Dev.* **14**: 2819-2830.

22.   Mitro, N., P. A. Mak, L. Vargas, C. Godio, E. Hampton, V. Molteni, A. Kreusch, and E. Saez. 2007. The nuclear receptor LXR is a glucose sensor. *Nature.* **445**: 219-223.

23.   Anthonisen, E. H., L. Berven, S. Holm, M. Nygard, H. I. Nebb, and L. M. Gronning-Wang. 2010. Nuclear receptor liver X receptor is O-GlcNAc-modified in response to glucose. *J. Biol. Chem.* **285**: 1607-1615.

24.   Miyazaki, M., A. Dobrzyn, W. C. Man, K. Chu, H. Sampath, H. J. Kim, and J. M. Ntambi. 2004. Stearoyl-CoA desaturase 1 gene expression is necessary for fructose-mediated induction of lipogenic gene expression by sterol regulatory element-binding protein-1c-dependent and -independent mechanisms. *J. Biol. Chem.* **279**: 25164-25171.

25.   Dentin, R., J. P. Pegorier, F. Benhamed, F. Foufelle, P. Ferre, V. Fauveau, M. A. Magnuson, J. Girard, and C. Postic. 2004. Hepatic glucokinase is required for the synergistic action of ChREBP and SREBP-1c on glycolytic and lipogenic gene expression. *J. Biol. Chem.* **279**: 20314-20326.

26. Henin, N., M. F. Vincent, H. E. Gruber, and G. Van den Berghe. 1995. Inhibition of fatty acid and cholesterol synthesis by stimulation of AMP-activated protein kinase. *FASEB. J.* **9**: 541-546.

27. Carling, D., P. R. Clarke, V. A. Zammit, and D. G. Hardie. 1989. Purification and characterization of the AMP-activated protein kinase. Copurification of acetyl-CoA carboxylase kinase and 3-hydroxy-3-methylglutaryl-CoA reductase kinase activities. *Eur. J. Biochem.* **186**: 129-136.

28. Zhang, X., X. Xie, B. L. Heckmann, A. M. Saarinen, T. A. Czyzyk, and J. Liu. 2014. Targeted disruption of G0/G1 switch gene 2 enhances adipose lipolysis, alters hepatic energy balance, and alleviates high-fat diet-induced liver steatosis. *Diabetes.* **63**: 934-946.

29. Wang, C., Y. Zhao, X. Gao, L. Li, Y. Yuan, F. Liu, L. Zhang, J. Wu, P. Hu, X. Zhang, Y. Gu, Y. Xu, Z. Wang, Z. Li, H. Zhang, and J. Ye. 2015. Perilipin 5 improves hepatic lipotoxicity by inhibiting lipolysis. *Hepatology.* **61**: 870-882.

30. Kaushik, S., and A. M. Cuervo. 2015. Degradation of lipid droplet-associated proteins by chaperone-mediated autophagy facilitates lipolysis. *Nat. Cell. Biol.* **17**: 759-770.

31. Reid, B. N., G. P. Ables, O. A. Otlivanchik, G. Schoiswohl, R. Zechner, W. S. Blaner, I. J. Goldberg, R. F. Schwabe, S. C. Chua, Jr., and L. S. Huang. 2008. Hepatic overexpression of hormone-sensitive lipase and adipose triglyceride lipase promotes fatty acid oxidation, stimulates direct release of free fatty acids, and ameliorates steatosis. *J. Biol. Chem.* **283**: 13087-13099.

32. Duncan, R. E., M. Ahmadian, K. Jaworski, E. Sarkadi-Nagy, and H. S. Sul. 2007. Regulation of lipolysis in adipocytes. *Annu. Rev. Nutr.* **27**: 79-101.

33. Gao, G., F. J. Chen, L. Zhou, L. Su, D. Xu, L. Xu, and P. Li. 2017. Control of lipid droplet fusion and growth by CIDE family proteins. *Biochim. Biophys. Acta.* **1862**: 1197-1204.

34. Li, J. Z., J. Ye, B. Xue, J. Qi, J. Zhang, Z. Zhou, Q. Li, Z. Wen, and P. Li. 2007. Cideb regulates diet-induced obesity, liver steatosis, and insulin sensitivity by controlling lipogenesis and fatty acid oxidation. *Diabetes.* **56**: 2523-2532.

20

35. Zhou, L., L. Xu, J. Ye, D. Li, W. Wang, X. Li, L. Wu, H. Wang, F. Guan, and P. Li. 2012. Cidea promotes hepatic steatosis by sensing dietary fatty acids. *Hepatology.* **56**: 95-107.

36. Langhi, C., and A. Baldan. 2015. CIDEC/FSP27 is regulated by peroxisome proliferator-activated receptor alpha and plays a critical role in fasting- and diet-induced hepatosteatosis. *Hepatology.* **61**: 1227-1238.

37. Maekawa, R., Y. Seino, H. Ogata, M. Murase, A. Iida, K. Hosokawa, E. Joo, N. Harada, S. Tsunekawa, Y. Hamada, Y. Oiso, N. Inagaki, Y. Hayashi, and H. Arima. 2017. Chronic high-sucrose diet increases fibroblast growth factor 21 production and energy expenditure in mice. *J. Nutr. Biochem.* **49**: 71-79.

38. von Holstein-Rathlou, S., L. D. BonDurant, L. Peltekian, M. C. Naber, T. C. Yin, K. E. Claflin, A. I. Urizar, A. N. Madsen, C. Ratner, B. Holst, K. Karstoft, A. Vandenbeuch, C. B. Anderson, M. D. Cassell, A. P. Thompson, T. P. Solomon, K. Rahmouni, S. C. Kinnamon, A. A. Pieper, M. P. Gillum, and M. J. Potthoff. 2016. FGF21 Mediates Endocrine Control of Simple Sugar Intake and Sweet Taste Preference by the Liver. *Cell. Metab.* **23**: 335-343.

39. Basaranoglu, M., G. Basaranoglu, and E. Bugianesi. 2015. Carbohydrate intake and nonalcoholic fatty liver disease: fructose as a weapon of mass destruction. *Hepatobiliary. Surg. Nutr.* **4**: 109-116.

40. Donnelly, K. L., C. I. Smith, S. J. Schwarzenberg, J. Jessurun, M. D. Boldt, and E. J. Parks. 2005. Sources of fatty acids stored in liver and secreted via lipoproteins in patients with nonalcoholic fatty liver disease. *J. Clin. Invest.* **115**: 1343-1351.

41. Schwarz, J. M., P. Linfoot, D. Dare, and K. Aghajanian. 2003. Hepatic de novo lipogenesis in normoinsulinemic and hyperinsulinemic subjects consuming high-fat, low-carbohydrate and low-fat, high-carbohydrate isoenergetic diets. *Am. J. Clin. Nutr.* **77**: 43-50.

42. Hudgins, L. C., C. E. Seidman, J. Diakun, and J. Hirsch. 1998. Human fatty acid synthesis is reduced after the substitution of dietary starch for sugar. *Am. J. Clin. Nutr.* **67**: 631-639.

21

43.   Carling, D., V. A. Zammit, and D. G. Hardie. 1987. A common bicyclic protein kinase cascade inactivates the regulatory enzymes of fatty acid and cholesterol biosynthesis. *FEBS. lett.* **223**: 217-222.

44.   Sato, R., J. L. Goldstein, and M. S. Brown. 1993. Replacement of serine-871 of hamster 3-hydroxy-3-methylglutaryl-CoA reductase prevents phosphorylation by AMP-activated kinase and blocks inhibition of sterol synthesis induced by ATP depletion. *Proc. Natl. Acad. Sci. U. S. A.* **90**: 9261-9265.

45.   Scott, J. W., D. G. Norman, S. A. Hawley, L. Kontogiannis, and D. G. Hardie. 2002. Protein kinase substrate recognition studied using the recombinant catalytic domain of AMP-activated protein kinase and a model substrate. *J. Mol. Biol.* **317**: 309-323.

46.   Woods, A., J. R. Williams, P. J. Muckett, F. V. Mayer, M. Liljevald, Y. M. Bohlooly, and D. Carling. 2017. Liver-Specific Activation of AMPK Prevents Steatosis on a High-Fructose Diet. *Cell. Rep.* **18**: 3043-3051.

47.   Kaushik, S., and A. M. Cuervo. 2016. AMPK-dependent phosphorylation of lipid droplet protein PLIN2 triggers its degradation by CMA. *Autophagy.* **12**: 432-438.

48.   Lian, J., R. Nelson, and R. Lehner. 2018. Carboxylesterases in lipid metabolism: from mouse to human. *Protein. Cell.* **9**: 178-195.

49.   Wei, E., Y. Ben Ali, J. Lyon, H. Wang, R. Nelson, V. W. Dolinsky, J. R. Dyck, G. Mitchell, G. S. Korbutt, and R. Lehner. 2010. Loss of TGH/Ces3 in mice decreases blood lipids, improves glucose tolerance, and increases energy expenditure. *Cell. Metab.* **11**: 183-193.

50.   Lian, J., E. Wei, S. P. Wang, A. D. Quiroga, L. Li, A. D. Pardo, J. van der Veen, S. Sipione, G. A. Mitchell, and R. Lehner. 2012. Liver specific inactivation of carboxylesterase 3/triacylglycerol hydrolase decreases blood lipids without causing severe steatosis in mice. *Hepatology.* **56**: 2154-2162.

51.   Lian, J., W. Bahitham, R. Panigrahi, R. Nelson, L. Li, R. Watts, A. Thiesen, M. J. Lemieux, and R. Lehner. 2018. Genetic variation in human carboxylesterase CES1 confers resistance to hepatic steatosis. *Biochim. Biophys. Acta.* **1863**: 688-699.

52.   Ferramosca, A., A. Conte, F. Damiano, L. Siculella, and V. Zara. 2014. Differential effects of high-carbohydrate and high-fat diets on hepatic lipogenesis in rats. *Eur. J. Nutr.* **53**: 1103-1114.
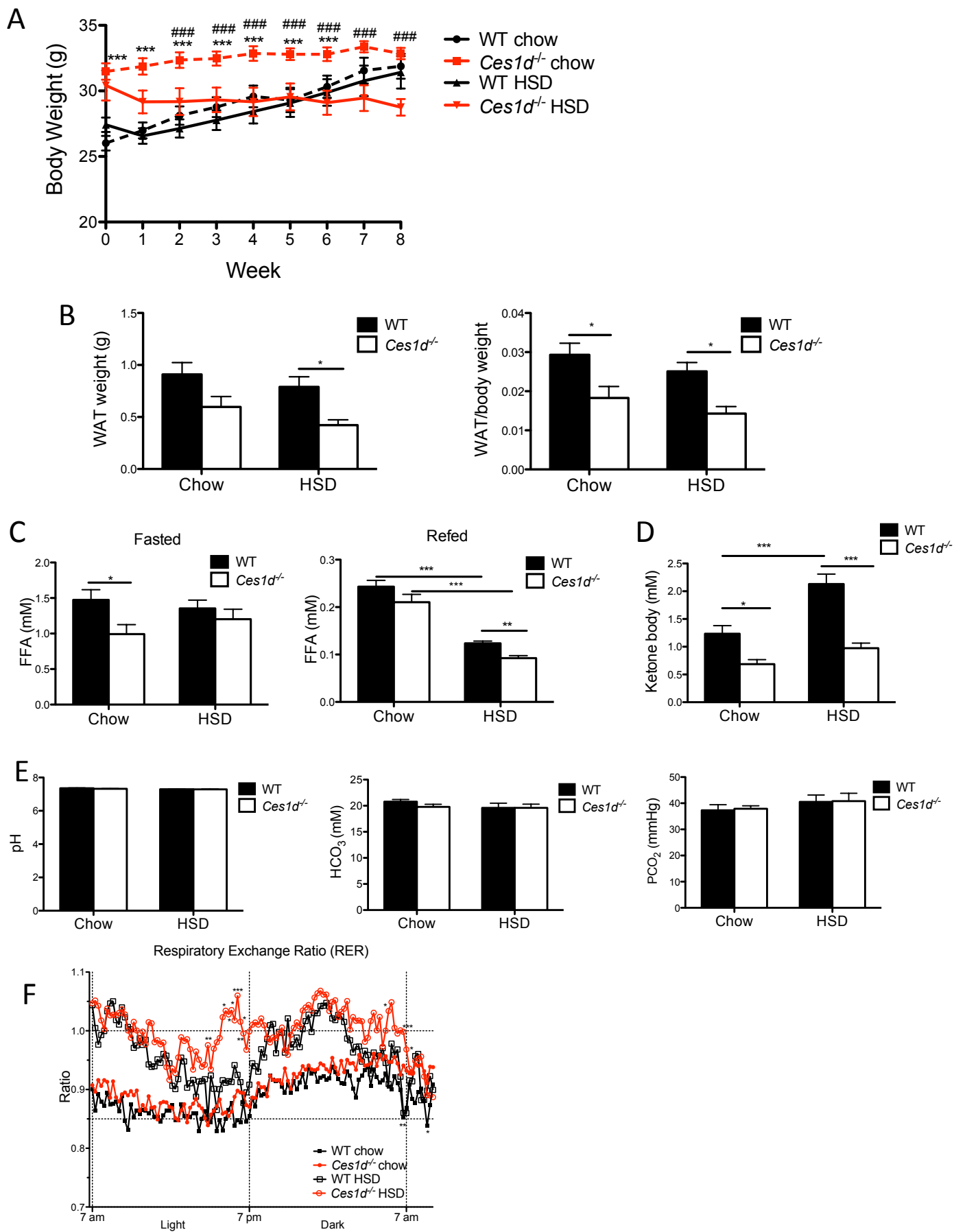
Figure 1. Effects of HSD and Ces1d deficiency on whole body metabolism. (A) Body weight of WT and *Ces1d⁻/⁻* mice fed either chow or HSD for 8 weeks. N=6, values are mean ± SEM. *P<0.05, **P<0.01, ***P<0.001 vs WT group on the same diet condition, $^{\#}$P < 0.05, $^{\#\#}$P < 0.01, $^{\#\#\#}$P < 0.001 vs HSD fed group in the same genotype. (B) Epididymal white adipose tissue (WAT) weight and WAT/body weight ratio of WT and *Ces1d⁻/⁻* mice fed either chow or HSD for 8 weeks. (C) Plasma free fatty acid concentrations in fasted and refed WT and *Ces1d⁻/⁻* mice fed either chow or HSD for 8 weeks. (D) Fasted plasma ketone body concentration in WT and *Ces1d⁻/⁻* mice fed either chow or HSD for 8 weeks. (E) Blood acid-base measurements after fasting in WT and *Ces1d⁻/⁻* mice fed either chow diet or HSD for 8 weeks. N=6-7, values are mean ± SEM. *P<0.05, ***P<0.001. (F) Respiratory exchange ratio (RER) of WT and *Ces1d⁻/⁻* mice fed either chow or HSD. N=6. *P<0.05, **P<0.01, ***P<0.001 for significance between groups in the same diet condition.
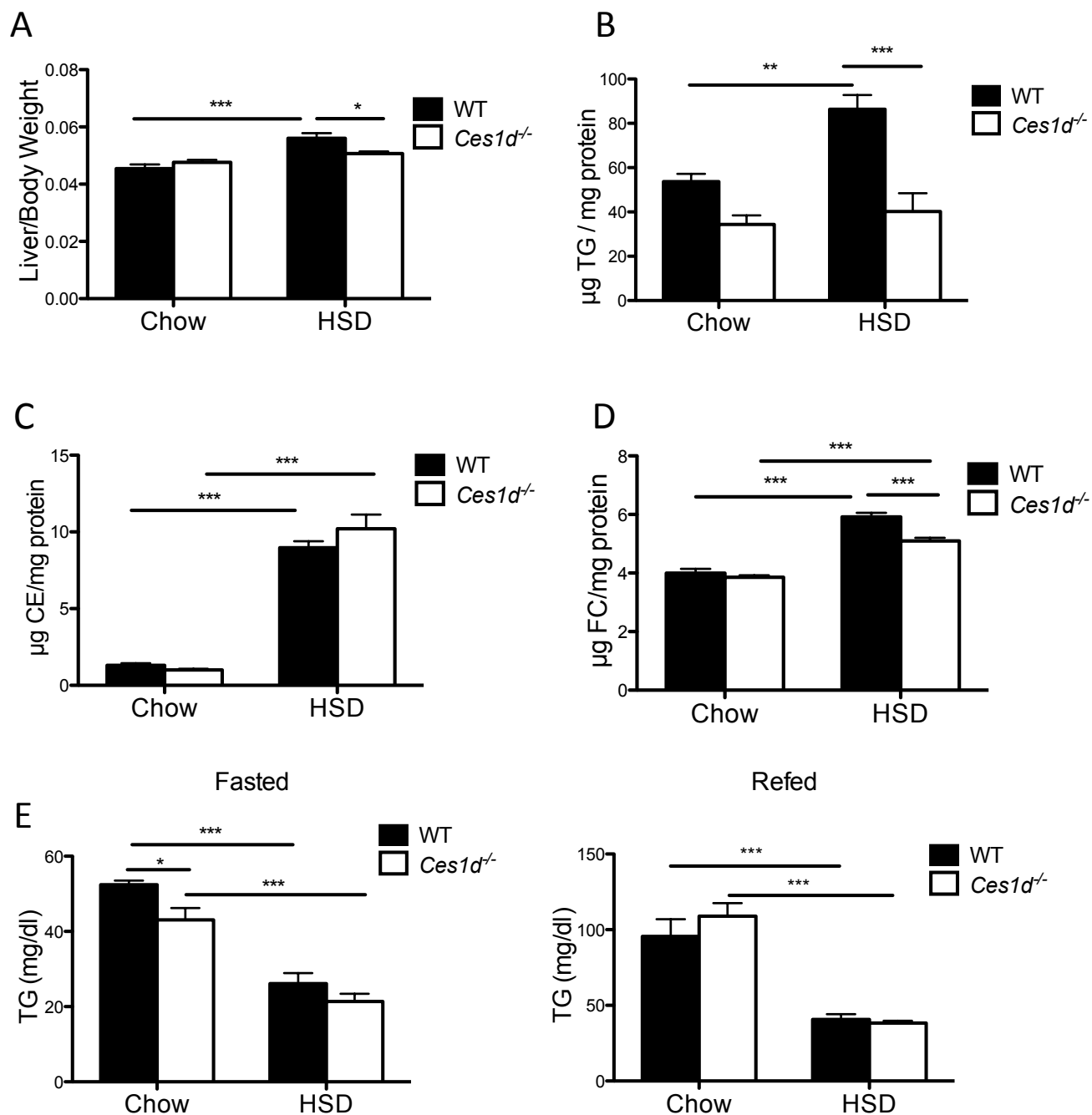
Figure 2. Ces1d deficiency ameliorated HSD-induced liver lipid accumulation. (A) Liver and body weight ratio of WT and *Ces1d⁻/⁻* mice fed either chow or HSD for 8 weeks. (B) Liver TG, (C) CE, and (D) FC concentrations in WT and *Ces1d⁻/⁻* mice fed either chow or HSD for 8 weeks. (E) Plasma TG concentrations in WT and *Ces1d⁻/⁻* mice fed either chow or HSD for 8 weeks. N=6, values are mean ± SEM. *P<0.05, **P<0.01, ***P<0.001.
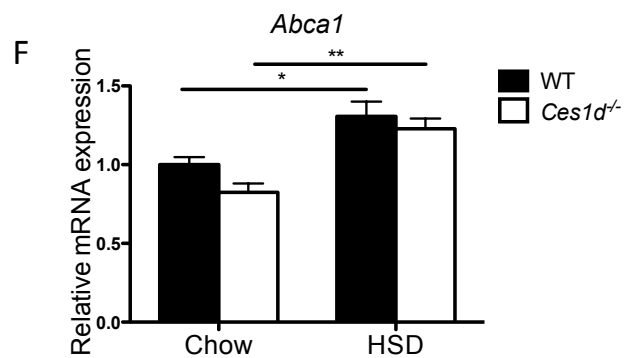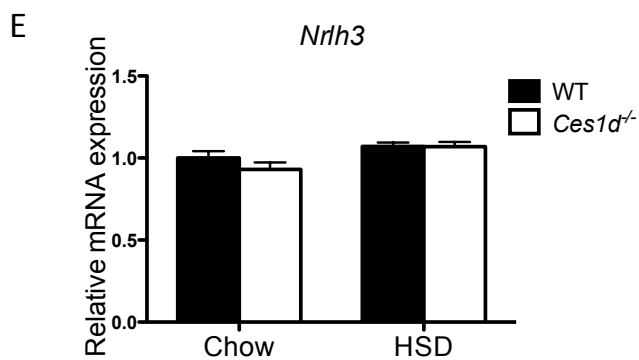
A

Mlxipl (alpha)

B

Mlxipl (beta)

C

Pklr

D

Txnip

E

Nrlh3

F

Abca1

G

Srebf1c
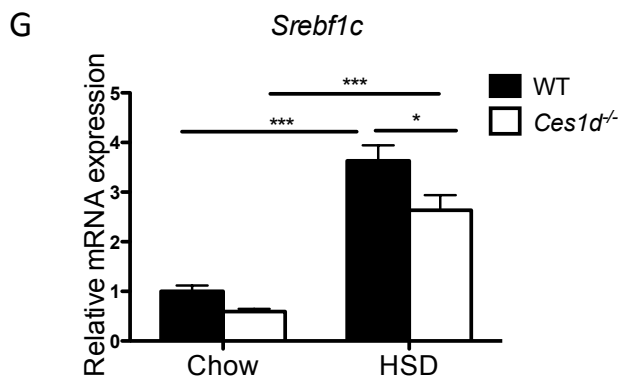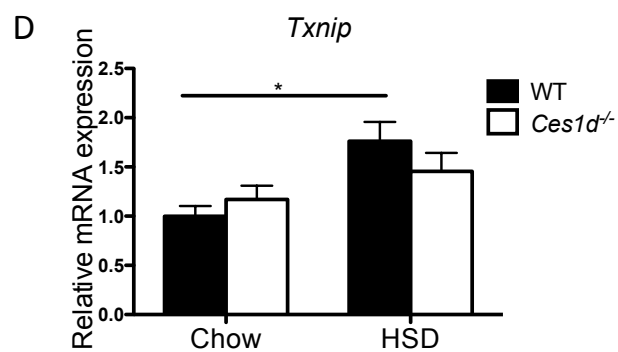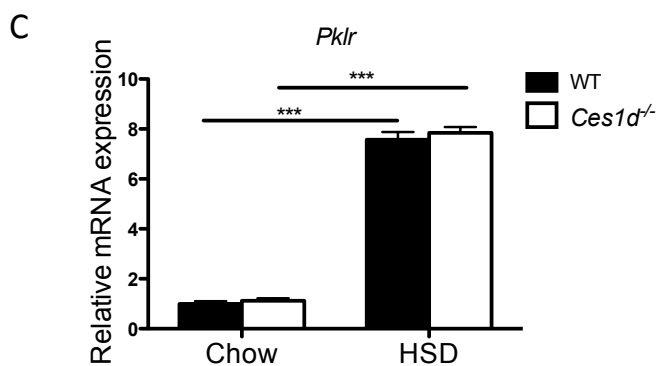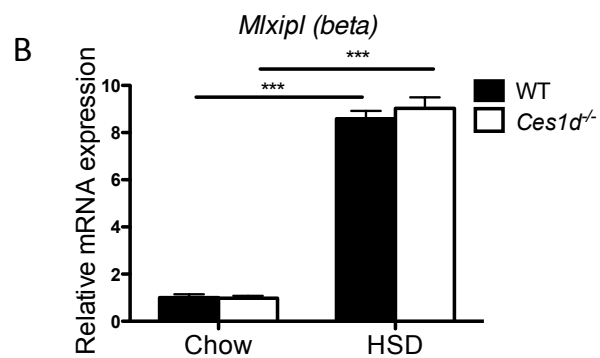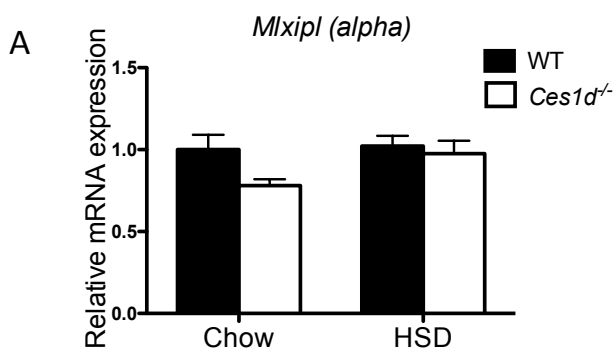
Figure 3. Effects of HSD and Ces1d deficiency on hepatic expression of lipogenic and lipid efflux regulatory genes. Hepatic mRNA expression of (A) *Mlxipl (alpha)*, (B) *Mlxipl (beta)*, ChREBP targets (C) *Pklr* and (D) *Txnip*, (E) *Nrlh3* and (F) LXRα target *Abca1*, and (G) *Srebf1c* in WT and *Ces1d*^{-/-} mice fed either chow or HSD for 8 weeks. N=6. Values are mean ± SEM. *P<0.05, **P<0.01, ***P<0.001.
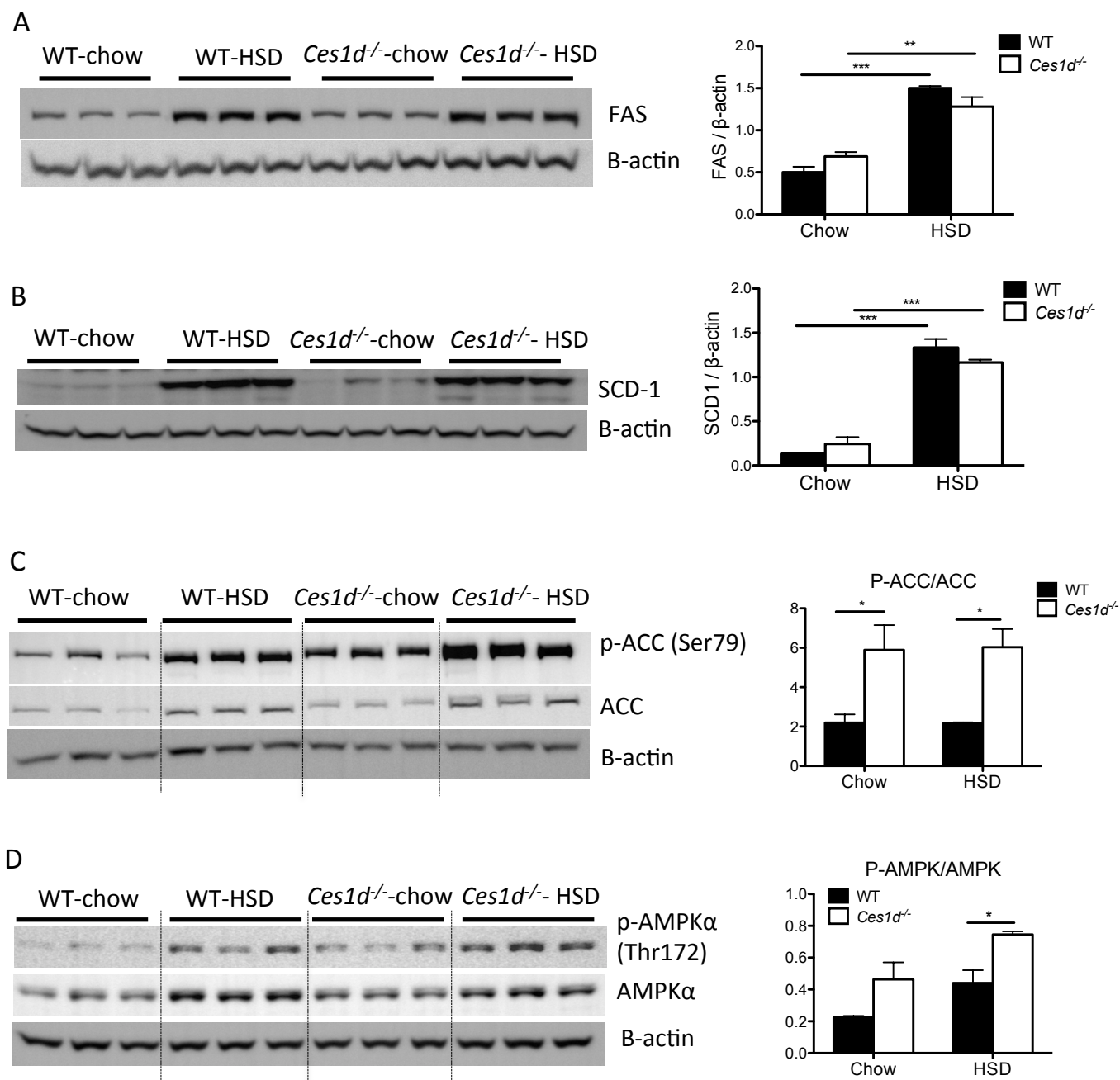
A

B

C

D

Figure 4. Effects of HSD and Ces1d deficiency on regulatory hepatic lipogenic enzymes and AMPK.

Abundance of liver (A) FAS, (B) SCD-1, (C) p-ACC/ACC, and (D) p-AMPK/AMPK in chow or HSD fed

WT and $Ces1d^{-/-}$ mice was assessed by immunoblotting. Values of relative band intensities were shown as
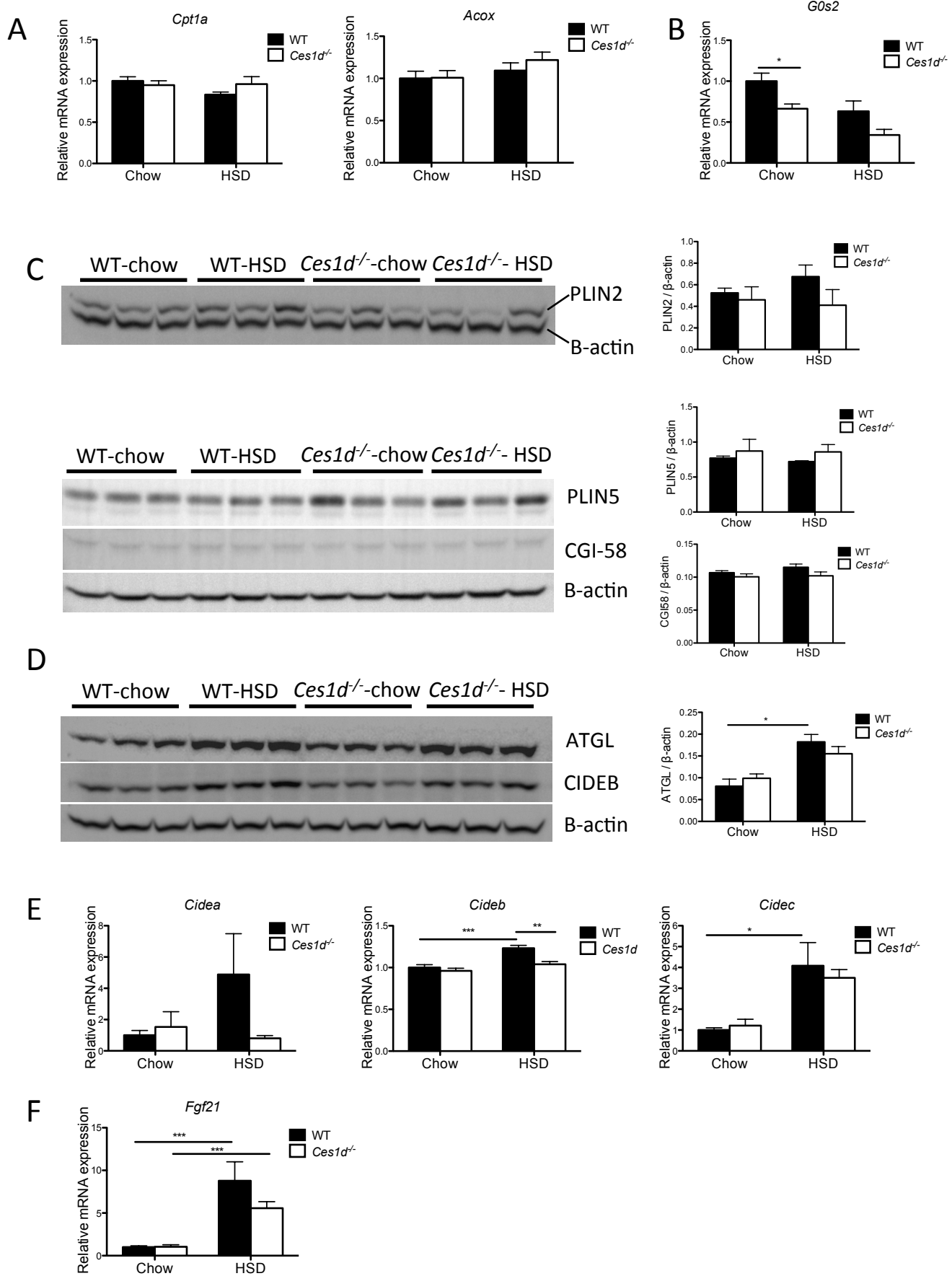
mean ± SEM. *P<0.05, **P<0.01, ***P<0.001.

Figure 5. Effects of HSD and Ces1d deficiency on regulatory hepatic lipid droplet metabolic genes/ enzymes. (A) Hepatic mRNA expression of genes involved in FA oxidation in fasted WT and *Ces1d$^{-/-}$* mice (n=6). (B) Hepatic mRNA expression of ATGL inhibitor *G0s2* (n=6). (C) Protein abundance of perilipin 2 (PLIN2), perilipin 5 (PLIN5), and ATGL coactivator CGI-58 in the liver of WT and *Ces1d$^{-/-}$* mice was assessed by immunoblotting. (D) Protein abundance of ATGL and lipid droplet (LD)-associated protein CIDEB in the liver of WT and *Ces1d$^{-/-}$* mice was assessed by immunoblotting. (E) Hepatic mRNA expression of LD-associated proteins CIDEA, CIDEB, and CIDEC (n=6). (F) Hepatic mRNA expression of *Fgf21* (n=6). Values are mean ± SEM. *P<0.05, **P<0.01, ***P<0.001.
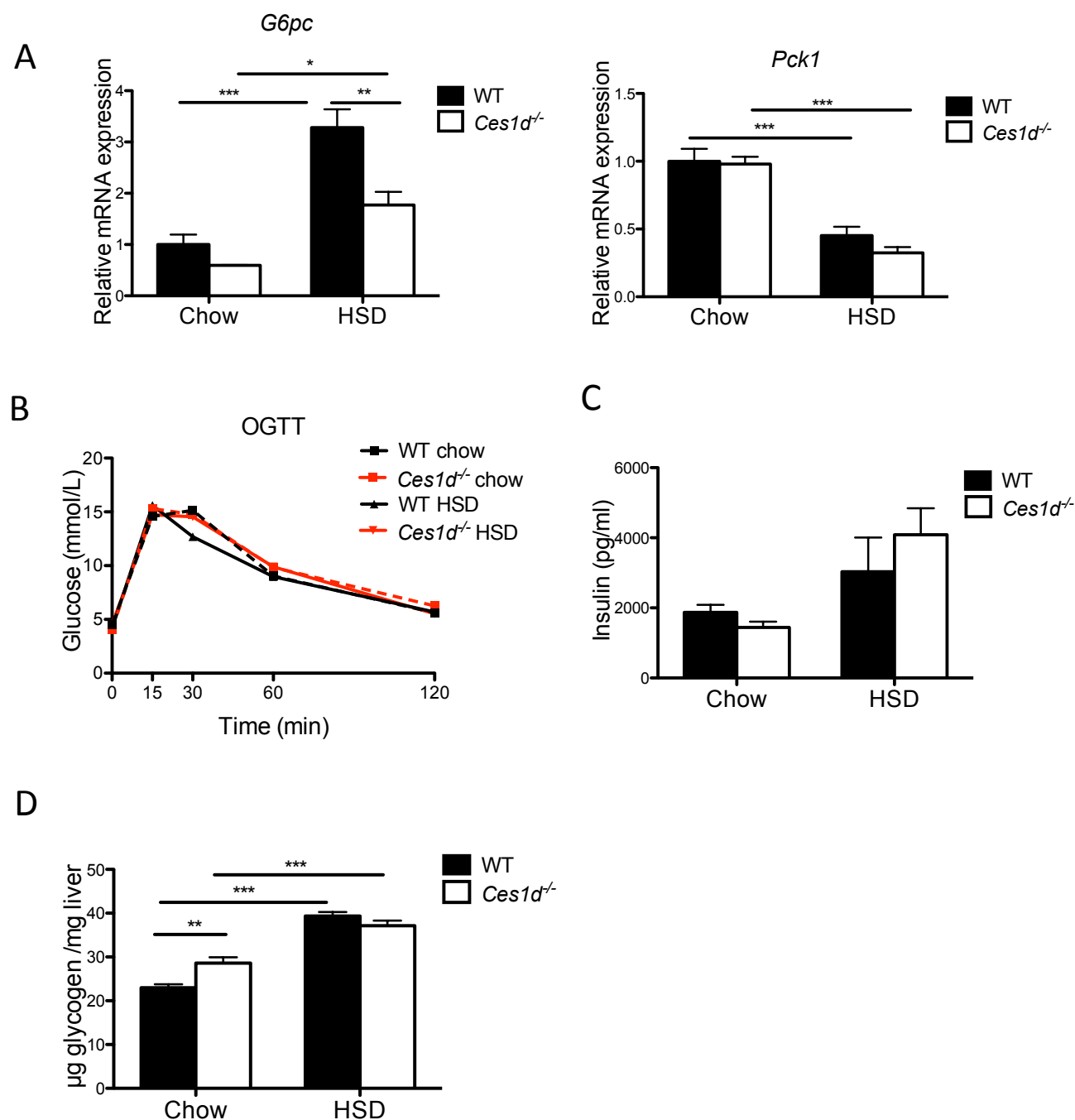
Figure 6. Effects of HSD and Ces1d deficiency on glucose metabolism. (A) Hepatic mRNA expression of key enzymes of gluconeogenesis in WT and *Ces1d*^{-/-} mice (n=6). (B) Glucose tolerance test (OGTT) in WT and *Ces1d*^{-/-} mice fed either chow or HSD (n=5-8). (C) Plasma insulin concentration after refeeding in WT and *Ces1d*^{-/-} mice fed either chow or HSD for 8 weeks (n=6). (D) Liver glycogen after refeeding in WT and *Ces1d*^{-/-} mice fed either chow or HSD for 8 weeks (n=6). Values are mean ± SEM. *P<0.05, **P<0.01, ***P<0.001.